Egyptian Knowledge Bank

International Journal of
Materials Technology and Innovation
Volume 5, Issue 1 (2025), pages 22-30

IJMTI

Online ISSN 2682-4299

Artificial Neural Network Prediction of Corrosion Rate in Friction Stir-Welded Aluminum Flange

Ibrahim Sabry*, Tarek El-Attar, Noah E. El-Zathry, A.M. Hewidy

[1] Department of Mechanical Engineering, Benha Faculty of Engineering, Benha University, Benha, Egypt

*Corresponding author: E-mail: ibrahim.sabry@bhit.bu.edu.eg (Ibrahim Sabry)

Received…….1 February 2025
Accepted…....….11 April 2025
Published……..…30 June 2025

Abstract

Expanding the application of the 6xxx aluminium alloy series across different industries presents challenges, particularly regarding the need for cost-effective welding techniques and optimal configurations to achieve high-quality joints. This research compared the joint performance of pipes and plates manufactured using friction stir welding (FSW). The AA6082 alloy was utilized for both the pipes and plates involved in the study. This article outlines a methodical procedure for enhancing the aluminium alloy by applying FSW variables. FSW is frequently used to challenge welding connections for aluminium alloys. Welding input parameters primarily determine the weld quality. The rate of joint corrosion is greatly influenced by welding factors such as shoulder diameter, rotating speed, and welding speed. The aluminium alloy 6082 by FSW has been attempted to be joined in the current work utilizing a standard milling machine. FSW was done on 6082 aluminium alloy plates that are 10 mm thick, pipes with a 53 mm outer diameter and a 4 mm wall thickness. Artificial neural networks (ANNs) have been created to predict the corrosion rate in FSW based on backpropagation (BP) of error. The tool diameter of the shoulder, the rotational speed of the tool, and the speed of welding are the model input parameters. The model output is the joint corrosion rate. Following that, the ANN was trained in utilizing experimental data. The ANN was tested by utilizing data from experiments, not through training. The findings indicated that the constructed neural network could be used as a potential method for determining the corrosion rate for specified process parameters, as the ANN results perfectly harmonized with the experimental data.

Keywords: Friction Stir Welding, Flange, Artificial Neural Networks, Corrosion Rate.

1. Introduction

Flange welding is a vital step in creating pipe networks. It's used to connect pipe components and repair damaged sections, allowing for the development of larger plumbing systems. Executing flange welding successfully requires a skilled welder who can navigate the various technical aspects. Welders are essential in the petrochemical industry, where their expertise is highly sought [1]. Welding is the key technique for effectively joining flanges, and mastering this skill is crucial since flanges serve as connectors for different pipe sections. This article demonstrates the best practices for welding flanges.

The ring-type joint flange is a top choice for high-pressure applications due to its ease of installation and compatibility with multiple flange types. When selecting a welding technique to attach the flange to the pipe, considerations such as base metal and flange type typically come into play. Nevertheless, the welding process remains similar to other commonly used methods [2,3].

To create a solid joint at the neck and lap junction between the pipe and the flange, you'll want to maintain a 1/16 to 1/8-inch gap. The first pass should penetrate the wall of both the pipe and flange assembly evenly to ensure a strong connection. The final pass should be approximately 1/16 inch larger than the outside diameter of the pipe [1].

This method is highly regarded for its ability to produce a dependable joint that stands the test of time for users. It performs well under varying pressures and temperatures. When using slip-on flanges, it's essential to remember that the final products may need to be re-grinded after welding. This technique is generally more labour- and cost-intensive than the traditional welding neck connection method, mainly due to the extra step of regrinding the completed pipe and flange. It's typically employed when a flawless, pit-free hole is required [1].

Tungsten Inert Gas (TIG) welding is the top choice for threaded flange connections because of its outstanding results. Manual orbital TIG welding is favoured for flange joints and similar setups, such as tube-to-tube sheet joints in shell and tube heat exchangers. Since flange and tube-to-tube sheet configurations can be intricate to weld, an experienced welder is needed. Using this welding technique requires the expertise of a skilled craftsman to create strong connections between the parts, ensuring there are no weak spots around the joint [4].

Fusion welding methods, including TIG and MIG, produce higher temperatures than the solid-state Friction Stir Welding (FSW) process. While fusion arc welding techniques reach temperatures that exceed the melting point of the base material, FSW does not require the same level of heat; instead, it needs a temperature above the recrystallization point. This modern solid-state welding technique avoids melting the base material entirely using a non-consumable [3].

Joining using a solid-state technique as FSW avoids melting and recasting the joined material. The FSW technique was developed in 1991 by The Welding Institute (TWI), UK. With this method, materials formerly conceived to be complicated to weld, as they tend to form melting flaws, can now be joined quickly. Over fusion welding, it has been found that the FSW technique offers several benefits [1]. Friction Stir Welding is inherently a stochastic process, akin to various fusion welding techniques, as it involves multiple factors that can affect the welding process. This complexity creates some uncertainty regarding the final characteristics of the weld, such as its quality and mechanical and metallurgical properties. Numerous studies have explored welding parameters, focusing on key factors such as rotational speed (N), linear speed (S), and plunging depth (D).

In addition to these basic parameters, other factors like dwell duration, vibrational frequency, and tool pin shape also play significant roles in the welding outcome. Research has examined these variables, yielding valuable insights. For example, in their study to improve the FSW of aluminium AA6063 pipes, Pawar and Sheet highlighted crucial parameters that influence mechanical qualities and microstructure. They discovered that a higher tool rotational speed (N) coupled with a lower welding speed (S) leads to enhanced FSW performance. Moreover, they noted that the shape of the pin significantly affects friction at the interface, which in turn impacts the properties of the joint.

Iftikhar et al. conducted extensive research on the weldability by FSW processes specifically for tube and tube-sheet configurations. Notably, a similar methodology was previously applied by Thekkuden et al. for creating leak-proof metallic tube-to-tube sheet joints.

Using material flow and friction heating, the non-consumable rotation tool produces defect-free FSW zones [2]. The FSW tool geometry and process parameters significantly impact the material flow behaviour. The effect of the speed of rotation, speed of welding, and diameter of the shoulder on the corrosion rate of Al 6063 aluminium alloy was investigated by El-Kassas et al. [3].

The impact of processing factors on the microstructural and mechanical characteristics of FS welded joints made from AA 6082 was examined by Sabry et al. [4]. To determine a correlation between FSW parameters and the mechanical characteristics of aluminium plates, Sabry et al. utilized an artificial neural network (ANN). Numerous studies [5-11] have looked into how different welding parameters of the process impact the durability of FS welded joints made of other materials. Researchers have occasionally tried optimizing friction stir welding parameters using various optimization models and solution methodologies. The current study aims to utilize ANN to forecast the corrosion rate in FSW. Expanding the applications of the 6xx aluminium alloy series across different industries presents challenges, particularly regarding the need for cost-effective welding techniques and optimal configurations to achieve high-quality joints. This research compares the joint performance of pipes and plates manufactured using friction stir welding (FSW). The AA6082 alloy was utilized for both the pipes and plates involved in the study.

This study explores the performance of flange joints prepared through friction stir welding (FSW) while incorporating artificial neural networks (ANN).

IJMTI vol. 5, issue 1 (2025) 22-30 https://doi.org/ 10.21608/IJMTI.2025.337737.1116

Three key factors are investigated: shoulder diameter, rotating speed, and welding speed, each assessed at three levels. The focus is on how these variables affect the corrosion rate. The selected process parameters obviously influence the characteristics of friction stir welded flange joints made from two identical aluminium alloys. The investigation is organized into two main parts. First, each process parameter is analysed to understand its effect on the flange joint's performance. Then, the strategies used to enhance and meticulously assess these effects are examined, with a particular emphasis on the role of ANN.

2. Experimental work

2.1 Preparation of Materials and Experimentation

For the current experimental investigations, a standard milling machine with a specially constructed fixture for FSW was used. The chemical makeup and mechanical characteristics of base metals are shown in Table 1. The welded joints were created using a non-consumable high-carbon, high-chromium steel tool known as K18 [10], as shown in Figs. 1 and 2. The FSW work was carried out at the Addis Machine Tool Industry, EEG, utilizing a Vertical Milling Machining Centre, as shown in Fig. 2. This machine features a spindle capable of operating at speeds ranging from 500 to 3000 RPM, with optimal settings for aluminium alloys typically between 1000 and 1800 RPM. A powerful spindle is essential to ensure consistent torque at lower speeds. The spindle motors deliver 30 kW of power, which is suitable for heavy-duty welding applications. The machines generally have a torque rating of around 400 Nm to handle demanding tasks.

Table 1: AL 6082 Composition and Properties.

	Al	**Si**	**Fe**	**Cu**	**Mn**	**Mg**	**Cr**	**Zn**	**Ti**
Wt. %	96	0.9	0.5	0.1	0.4	0.6	0.25	0.2	0.1

Ultimate tensile strength, MPa	**Hardness, HB**	**Elongation, %**
190	81	16

Additionally, the worktable provides ample space for flat plates used in FSW, with standard dimensions of 800 mm by 400 mm. The study's pipes and plates have an outer diameter of 53 mm, a wall thickness of 4 mm, and a plate thickness of 9 mm. They are both composed of the 6082- aluminum alloy. Table 1 shows the mechanical properties and chemical composition. Tests have been carried out to determine the parameters functional range.

The practical levels of parameters were selected to ensure the FSW joints have no obvious exterior flaws [12]. Twenty-seven experiments in total are performed, as stated in Table 2. With the aid of a CNC machine, the welded joints were first cut into the desired shapes. According to the ASTM G102 standard, three tensile samples have been created for all runs. A test using a three-electrode cell was used to determine the corrosion rate of the FSW joints, as shown in the following section.

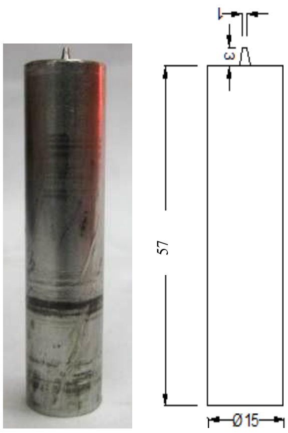

Fig. 1 The Tool's Geometric Specifications.

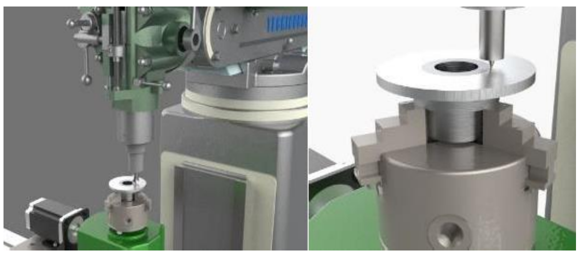

Fig. 2 The Fixture and Set Used to Induce FSW for a Flange in Schematic Form.

IJMTI vol. 5, issue 1 (2025) 22-30 https://doi.org/ 10.21608/IJMTI.2025.337737.1116

2.2 Electrochemical Analysis

Corrosion tests were conducted using a WENKING Mlab multichannel potentiostat and a SCI-Mlab corrosion monitoring system. The electrochemical setup included an Ag/AgCl reference electrode, a platinum plate counter electrode, and 6061 aluminum pipe specimens as the working electrodes. All tests were performed in a 3.5% NaCl solution with a pH of 6.8. Specimens for corrosion testing were prepared from the base metal, heat-affected zone (HAZ), and weldment.

Table 2: Tests and Findings.

Run	FSW process parameters			Corrosion rate mm/year
	N	D	S	CR
1	-1.000	-1.000	-1.000	2.307
2	-1.000	0.000	-1.000	2.672
3	-1.000	1.000	-1.000	3.118
4	-1.000	-1.000	0.000	1.329
5	-1.000	0.000	0.000	1.357
6	-1.000	1.000	0.000	1.873
7	-1.000	-1.000	1.000	1.076
8	-1.000	0.000	1.000	1.285
9	-1.000	1.000	1.000	1.623
10	0.000	-1.000	-1.000	1.1535
11	0.000	0.000	-1.000	1.336
12	0.000	1.000	-1.000	1.559
13	0.000	-1.000	0.000	0.6645
14	0.000	0.000	0.000	0.6785
15	0.000	1.000	0.000	0.9365
16	0.000	-1.000	1.000	0.538
17	0.000	0.000	1.000	0.6425
18	0.000	1.000	1.000	0.8115
19	1.000	-1.000	-1.000	1.307
20	1.000	0.000	-1.000	1.672
21	1.000	1.000	-1.000	2.118
22	1.000	-1.000	0.000	0.329
23	1.000	0.000	0.000	0.357
24	1.000	1.000	0.000	0.873
25	1.000	-1.000	1.000	0.076
26	1.000	0.000	1.000	0.285
27	1.000	1.000	1.000	0.623

2.3 MATLAB-Based ANN Modelling for FSW Corrosion Rate

Artificial neural networks (ANNs) are clever algorithms with biological inspiration. ANN has become increasingly popular in many engineering domains because of its intriguing qualities, including acquisition, generalization, fast processing, and ease of execution. ANNs typically consist of various straightforward and intricately coupled processing components arranged in layers [13].

MATLAB was used to create a multi-layer perception to estimate the pace of corrosion. Testing was done using experimental data that had not been used during training, which was used to train the BP first. Out of 27, 70% of the data were used for training, while 15% were used for testing and cross-validation. The following equation [13] normalizes the input and output data from 0.1 to 0.9. Modelling Data Using Networks and ANN Application Methodology

No precise mathematical model can accurately capture most industrial processes' behaviour since these processes are complicated, highly nonlinear, and need many input variables. In process modelling for monitoring and control, intelligent sensors are utilized to estimate variables that are generally unmeasurable online, in dynamic system identification, fault detection and diagnosis, and ultimately, in process control, artificial neural networks have found many applications because they are affordable, simple to understand, and capable of learning from examples [14].

Various applications use artificial neural networks (ANNs), computational models that simulate the operation of biological networks made up of neurons. The system has four layers: input, two concealed, and output. Each input factor is part of the input layer [15]. The output vector is produced in the final layer following the data processing from the input layer through two hidden layers. Simple synchronous processing components, modelled after the biological nervous systems, make up neural networks. The neuron is the fundamental component of the ANN [16].

The linkages between neurons are referred to as synapses, and each one of these synapses has a weight. There are more places where information on the neural network modelling approach is presented. The training process runs five iterations for each network architecture with various random beginning biases and weights. A network with two hidden layers that had been trained demonstrated reasonable performance indications after comparing the effectiveness of multiple architectures. Figure 3 depicts the network

IJMTI vol. 5, issue 1 (2025) 22-30 https://doi.org/ 10.21608/IJMTI.2025.337737.1116

architecture that was created. Thus, the network architecture has two input neurons, nine hidden neurons, and a nonlinear activation function. A single neuron with a linear activation function. The trained network weights and biases are displayed in Table 3.

2.4 Simulation of Neural Network

This study aimed to show that employing neural networks to calculate the mechanical parameters of welded Al flanges utilizing the FSW approach is feasible. The findings indicated that networks can be used in these systems instead of other techniques. The Levenberg-Marquardt algorithm performs better for the suggested NN model because it approximates the performance index using a second-order Taylor series instead of an approximate order as with the gradient descent algorithm. It was discovered that there was agreement in the correlations between the measured and projected correlation rate values.

APE = (Predicted - Actual) / (Actual) ×100[16](1)

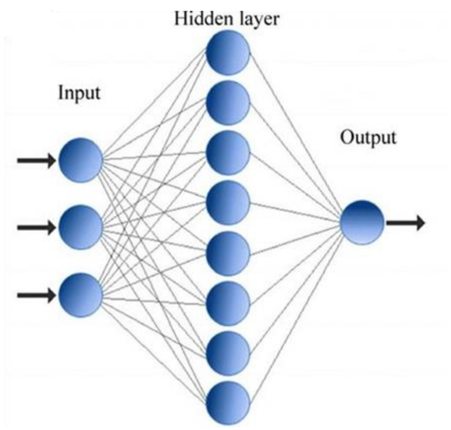

Fig. 3 Design of a Neural Network for FSW

3. Results and discussion

The corrosion behaviour of friction stir welded (FSW) joints is significantly influenced by process parameters such as rotation speed, travel speed, and shoulder diameter. These parameters determine the microstructural characteristics of the weld, which in turn affect corrosion resistance. Below is a discussion of how each parameter influences the corrosion rate in friction-stir welded aluminium alloys. Rotation speed plays a crucial role in heat generation and material flow during FSW, with a higher rotation speed (1800 RPM). This leads to higher heat input, which results in grain coarsening in the nugget zone (NZ). This can accelerate intermetallic compound (IMC) formation and oxide inclusion, increasing corrosion susceptibility. However, excessive heat may reduce residual stresses, slightly improving corrosion resistance, Fig. 5. Moderate rotation speed (1400 RPM) produces a balanced grain structure, reducing susceptibility to corrosion. Less thermal input minimizes IMC thickness, leading to improved corrosion resistance.

Table 3 presents a lower rotation speed (1000 RPM), which generates less heat, leading to insufficient material flow and potential defects such as voids or tunnel defects. These defects create localized corrosion sites, increasing the overall corrosion rate. Very high or very low rotation speeds may increase the corrosion rate, while a moderate speed (1400 RPM) results in a more uniform grain structure, reducing corrosion susceptibility.

Travel speed influences heat input per unit length and the degree of plastic deformation in the welded region. Low travel speed (2 mm/min): It produces high heat input, producing grain coarsening and thicker IMC layers at the interface—the corrosion rate increases due to the formation of a heterogeneous microstructure.

Moderate travel speed (5 mm/min) Results in a well-balanced thermal profile, leading to fine equiaxed grains in the weld zone. This provides optimal corrosion resistance due to a more uniform microstructure. High travel speed (7 mm/min) leads to lower heat input, reducing IMC formation but increasing weld defects like incomplete fusion or tunnel defects. These defects can act as localized corrosion sites, slightly increasing the corrosion rate. Very low travel speed increases corrosion due to excessive IMC formation, while very high travel speed increases corrosion due to defects. The optimal travel speed for lower corrosion rates is around 5 mm/min.

The shoulder diameter affects the weld's material flow, heat input, and surface morphology. Smaller shoulder diameter (20 mm) generates lower heat input, which may lead to poor material mixing and weld defects such as porosity. These defects serve as preferential corrosion sites, increasing the corrosion rate. Moderate shoulder diameter (30 mm) Provides sufficient heat generation and uniform material flow, leading to a defect-free weld with fine grains. This ultimately results in an enhanced corrosion resistance compared to smaller and larger shoulder diameters.

IJMTI vol. 5, issue 1 (2025) 22-30 https://doi.org/ 10.21608/IJMTI.2025.337737.1116

Larger shoulder diameter (40 mm) produces excessive heat, leading to grain coarsening and forming thicker IMC layers. It may also cause surface oxidation, making the weld more prone to localized corrosion. A shoulder diameter of 30 mm provides the best balance between heat input and material flow, reducing corrosion susceptibility. Optimal FSW parameters for the lowest corrosion rate, 1400 rpm, travel speed: ~5 mm/min, and shoulder diameter: ~30 mm

Figure 5 displays the corrosion test results for the specimens. A graph with a higher negative value or potential indicates a higher corrosion rate. Table 3 shows the corrosion rate value obtained from tests on flange FSW samples conducted using the electrochemical method with a three-electrode cell device and the NOVA 1.11 software [17, 18]. Additionally, the flow characteristics of the material are also impacted by the pins utilized during the welding process [19-23].

The BP method with one hidden layer enhanced by the training function named Traingdx is employed in the current work. The ANN is tested and trained using the MATLAB platform. A hidden layer with more neurons (5–10) was used to specify the output precisely during training. The input parameters for the first layer of ANN include the diameter of the tool, speed of rotation, and speed of welding. The ANN layer of the outer layer measures how quickly welded components corrode. This network has been successfully trained and tested using known test data. Table 3 contains a list of the training settings employed in this experiment. Following successful training, the neural network reported in this study was utilized to forecast the corrosion rate of FS-welded joints within the taught range.

The measured and anticipated values of output in Table 3 are close. Artificial neural networks that feedforward manner were applied in every instance in the current study. The network's output is compared using statistical techniques. Errors that arise during the learning and testing stages are referred to by the words root-mean-square (RMS), absolute fraction of variance (R^2), and mean error percentage numbers.

According to Fig 4, the ultimate mean-square error is modest. Similar characteristics can be seen in both the test and validation set errors. At iteration 124, no appreciable overfit occurred. Figure 4 displays the linear regression between the network outputs and the related targets. In our situation, the training, testing, and validation output closely match the target, and the overall response's R^2-value is just over 0.981.

Table 3: Measured vs. Predicted values.

	INPUT			OUTPUT	Predicted Output
Run	N	S	D	CR	CR
1	-1.000	-1.000	-1.000	2.307	2.2298
2	-1.000	0.000	-1.000	2.672	2.6342
3	-1.000	1.000	-1.000	3.118	2.6356
4	-1.000	-1.000	0.000	1.329	1.2173
5	-1.000	0.000	0.000	1.357	1.5247
6	-1.000	1.000	0.000	1.873	1.8418
7	-1.000	-1.000	1.000	1.076	0.86438
8	-1.000	0.000	1.000	1.285	1.1995
9	-1.000	1.000	1.000	1.623	1.5446
10	-1.000	-1.000	-1.000	1.1535	1.0902
11	0.000	0.000	-1.000	1.336	1.1138
12	0.000	1.000	-1.000	1.559	1.5082
13	0.000	-1.000	0.000	0.6645	0.7051
14	0.000	0.000	0.000	0.6785	0.8621
15	0.000	1.000	0.000	0.9365	0.96276
16	0.000	-1.000	1.000	0.538	0.60183
17	0.000	0.000	1.000	0.6425	0.63029
18	0.000	1.000	1.000	0.8115	0.88228
19	1.000	-1.000	-1.000	1.307	0.96761
20	1.000	0.000	-1.000	1.672	0.80447
21	-1.000	1.000	-1.000	2.118	0.94338
22	1.000	-1.000	0.000	0.329	0.26058
23	1.000	0.000	0.000	0.357	0.31649
24	1.000	1.000	0.000	0.873	0.62161
25	1.000	-1.000	1.000	0.076	0.22756
26	1.000	0.000	1.000	0.285	0.27845
27	1.000	1.000	1.000	0.623	0.53122

The experimental variation and ANN predictions for the mechanical characteristics of the FSW Al flange. The measured and anticipated production values are incredibly similar. Less than 3% of the time between the experiment and the expected ANN architect 3-8-1 is lost. As a result, the train network may be utilized to forecast the tensile strength given the process parameters.

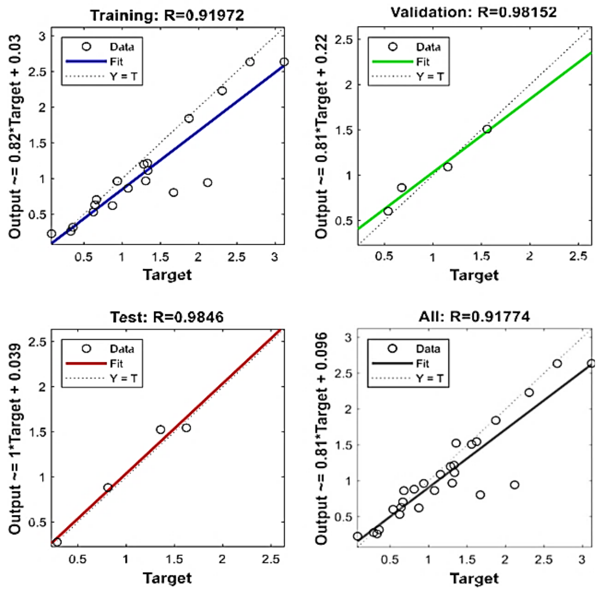

Fig. 4 Analysis of the Trained Network Performance.

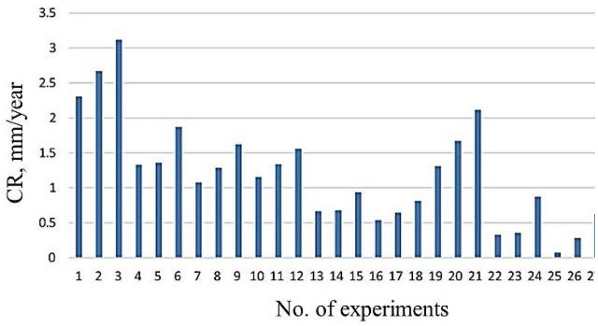

Fig. 5 Corrosion Rate Results.

Conclusions

For the specified FSW process parameters, the created neural network may be utilized to forecast the corrosion rate of the welded aluminium flange. Outcomes show that the forecast made by the network and the experiment outcomes are incredibly similar. The R-value is more significant than 0.981 overall for testing, validation, and training. It is discovered that the 3-8- 1 ANN architect's measurement and error anticipated values are fewer than 3%. The study offers hope for comprehending the friction stir welding procedure for attaching flanges and correlating the procedure's variables to the corrosion rate

References

[1] M.A. Wahid, Z.A. Khan, A.N. Siddiquee. Review on underwater friction stir welding: A variant of friction stir welding with great potential of improving joint properties, Transactions of Nonferrous Metals Society of China 28 (2018) 193–219. https://doi.org/10.1016/S1003-6326(18)64653-9.

[2] A.D. D'Souza, S.S. Rao, M.A. Herbert, Taguchi method of optimization of process variables for ultimate tensile strength of friction stir welded joint of Al-Ce-Si-Mg aluminium alloy plates, Mater Today Proc 46 (2021) 2691–2698. https://doi.org/10.1016/J.MATPR.2021.02.391.

[3] A.M. El-Kassas, I. Sabry, A.-H.I. Mourad, D.T. Thekkuden, A.M. El-Kassas, I. Sabry, A.-H.I. Mourad, D.T. Thekkuden, Characteristics of Potential Sources - Vertical Force, Torque and Current on Penetration Depth for Quality Assessment in Friction Stir Welding of AA 6061 Pipes, International Review of Aerospace Engineering (IREASE) 12 (2019) 195–204. https://doi.org/10.15866/IREASE.V12I4.16362.

[4] I. Sabry, N.E. El-Zathry, A.M. Hewidy, Experimental investigation on joining process of (plate to pipe) aluminum alloy 6082-T6 using friction stir welding, NILES 2022 - 4th Novel Intelligent and Leading Emerging Sciences Conference, Proceedings (2022) 360–363. https://doi.org/10.1109/NILES56402.2022.9942413.

[5] I. Sabry, A.M. El-Kassas, A.M. Khourshid, H.M. Hindawy, Comparison of RSM and RA with ANN in predicting mechanical properties of friction stir welded aluminum pipes, Engg. & Tech. in India 8 (n.d.) 1–14. https://doi.org/10.15740/HAS/ETI/8.1&2/1-14.

[6] A.M. El-Kassas, I. Sabry, A.M. Khourshid, I. Sabry, Integration between Artificial Neural Network and Responses Surface Methodology for Modeling of Friction Stir Welding Integration between Artificial Neural Network and Responses Surfaces Methodology for Modeling of Friction Stir welding, International Journal of Advanced Engineering Research and Science (IJAERS) 2 (2015). https://www.researchgate.net/publication/331966156 (accessed June 27, 2025).

[7] H.J. Liu, H.J. Zhang, Y.X. Huang, L. Yu, Mechanical properties of underwater friction

stir welded 2219 aluminum alloy, Transactions of Nonferrous Metals Society of China 20 (2010) 1387–1391. https://doi.org/10.1016/S1003-6326(09)60309-5.

[8] T.W. Nelson, R.J. Steel, W.J. Arbegast, In situ thermal studies and post-weld mechanical properties of friction stir welds in age hardenable aluminium alloys, Science and Technology of Welding and Joining 8 (2003) 283–288. https://doi.org/10.1179/136217103225011005.

[9] S.S. Sabari, S. Malarvizhi, V. Balasubramanian, The effect of pin profiles on the microstructure and mechanical properties of underwater friction stir welded AA2519-T87 aluminium alloy, International Journal of Mechanical and Materials Engineering 11 (2016) 1–14. https://doi.org/10.1186/S40712-016-0058-Y/FIGURES/8.

[10] S. Shanavas, J. Edwin Raja Dhas, N. Murugan, Weldability of marine grade AA 5052 aluminum alloy by underwater friction stir welding, International Journal of Advanced Manufacturing Technology 95 (2018) 4535–4546. https://doi.org/10.1007/S00170-017-1492-6/METRICS.

[11] K. Wang, J. Wu, W. Wang, L. Zhou, Z. Lin, L. Kong, Underwater friction stir welding of ultrafine grained 2017 aluminum alloy, Journal of Central South University 2012 19:8 19 (2012) 2081–2085. https://doi.org/10.1007/S11771-012-1248-2.

[12] I. Sabry, Experimental and statistical analysis of possibility sources - rotation speed, clamping torque and clamping pith for quality assessment in friction stir welding, Management and Production Engineering Review 12 (2021) 84–96. https://doi.org/10.24425/MPER.2021.138533

[13] I. Sabry, A.H.I. Mourad, D.T. Thekkuden, Study on Underwater Friction Stir Welded AA 2024-T3 Pipes Using Machine Learning Algorithms, ASME International Mechanical Engineering Congress and Exposition, Proceedings (IMECE) 2A-2021 (2022). https://doi.org/10.1115/IMECE2021-71378.

[14] L. Imani, A. Rahmani Henzaki, R. Hamzeloo, B. Davoodi, Modeling and optimizing of cutting force and surface roughness in milling process of Inconel 738 using hybrid ANN and GA, Proceedings of the Institution of Mechanical Engineers, Part B: Journal of Engineering Manufacture 234 (2020) 920–932. https://doi.org/10.1177/0954405419889204.

[15] M.H. Shojaeefard, R.A. Behnagh, M. Akbari, M.K.B. Givi, F. Farhani. Modelling and Pareto optimization of mechanical properties of friction stir welded AA7075/AA5083 butt joints using neural network and particle swarm algorithm, Materials & Design, 44 (2013) 190–198. https://doi.org/10.1016/J.MATDES.2012.07.025.

[16] H. Mohammadzadeh Jamalian, M. Tamjidi Eskandar, A. Chamanara, R. Karimzadeh, R. Yousefian. An artificial neural network model for multi-pass tool pin varying FSW of AA5086-H34 plates reinforced with Al2O3 nanoparticles and optimization for tool design insight, CIRP Journal of Manufacturing Science and Technology, 35 (2021) 69–79. https://doi.org/10.1016/J.CIRPJ.2021.05.007.

[17] S. Yadav, S. Gangwar, P.C. Yadav, V.K. Pathak, S. Sahu. Mechanical and corrosion behavior of SiC/Graphite/ZrO2 hybrid reinforced aluminum-based composites for marine environment, Surf Topogr 9 (2021) 045022. https://doi.org/10.1088/2051-672X/AC2F87.

[18] Q. Ding, H. Das, P. Upadhyay, B.C. Sousa, K. Karayagiz, A. Powell, B. Mishra. Microstructural, Corrosion, and Mechanical Characterization of Friction Stir Welded Al 6022-to-ZEK100 Mg Joints, Corrosion and Materials Degradation ,(4)(2023) 142–157. https://doi.org/10.3390/CMD4010009.

[19] F.H. Zamrudi, A.R. Setiawan. Effect of friction stir welding parameters on corrosion behaviour of aluminium alloys: an overview, Corrosion Engineering Science and Technology 57 (2022) 696–707. https://doi.org/10.1080/1478422X.2022.2116185.

[20] A. Laska, M. Szkodo, D. Koszelow, P. Cavaliere. Effect of Processing Parameters on Strength and Corrosion Resistance of Friction Stir-Welded AA6082, Metals (12) (2022) 192. https://doi.org/10.3390/MET12020192.

[21] Q. Wang, Y. Zhao, K. Yan, S. Lu. Corrosion behavior of spray formed 7055 aluminum alloy joint welded by underwater friction stir welding, Materials & Design, (68) (2015) 97–103.

https://doi.org/10.1016/J.MATDES.2014.12.019.

[22] I. Sabry. Exploring the effect of friction stir welding parameters on the strength of AA2024 and A356-T6 aluminum alloys, Journal of Alloys and Metallurgical Systems 8 (2024) 100124. https://doi.org/10.1016/J.JALMES.2024.100124.

[23] I. Sabry, A.M. Hewidy, M. Alkhedher, A.H.I. Mourad. Analysis of variance and grey relational analysis application methods for the selection and optimization problem in 6061-T6 flange friction stir welding process parameters, International Journal of Lightweight Materials and Manufacture 7 (2024) 773–792. https://doi.org/10.1016/J.IJLMM.2024.06.006.